Tome 39 N° 8 AOÛT 1978

LE JOURNAL DE PHYSIQUE

Classification
Physics Abstracts
24.10H

THE SENSITIVITY OF THE REAL PART OF THE NUCLEUS-NUCLEUS POTENTIAL TO NUCLEAR DENSITIES

Fl. STANCU

Université de Liège, Institut de Physique,
Sart Tilman, B-4000 Liège 1, Belgium

(*Reçu le 15 mars 1978, accepté le 14 avril 1978*)

Résumé. — On calcule la partie réelle du potentiel noyau-noyau à partir d'une méthode basée sur la fonctionnelle d'énergie de l'interaction nucléon-nucléon de Skyrme. On présente une description détaillée de la dépendance des résultats par rapport au choix des densités pour les neutrons et les protons.

Abstract. — We calculate the real part of the nucleus-nucleus potential by using a method based on the energy functional of the Skyrme nucleon-nucleon interaction and give a detailed account of the dependence of the results on the choice of the neutron and proton densities.

1. **Introduction.** — The elastic scattering data of two heavy ions give the value of the real part of the nucleus-nucleus interaction potential at the strong absorption radius [1, 2]. At such separations only the tails of the density distributions of the interacting nuclei overlap, and as a result the nuclear contribution represents only a small fraction of the whole interaction given by the sum of nuclear and coulomb potentials. This small contribution has a decisive role for the value of the grazing angle [2] and therefore calculations of the interaction potential should be based on nuclear densities which provide an accurate description of the region where the density becomes smaller than 10 % of its central value.

In a previous paper [3] we have calculated the real part of the nucleus-nucleus interaction potential from Skyrme's nucleon-nucleon interaction by using the energy density formalism developed by Vautherin and Brink [4] for spherical nuclei. Besides the Skyrme interaction parameters the calculation required the knowledge of the neutron and proton densities of the interacting nuclei. For simplicity the calculations of reference [3] were made using Fermi type distributions ρ_F adjusted to reproduce the Skyrme-Hartree-Fock densities ρ_{HF} of reference [5]. These Fermi type distributions are adjusted to reproduce the surface region of the Skyrme-Hartree-Fock densities but they are somewhat different from ρ_{HF} in the tail region i.e., where $\rho(r) < 0.1\ \rho(0)$. This difference might be significant for our calculations.

The purpose of the present work is twofold. First we study the validity of the approximation ρ_F (eq. (4)) for nucleus-nucleus potential calculations in the barrier region. For this purpose we perform calculations with ρ_{HF} and make a comparison with the results obtained in [3] from ρ_F. Second we examine the sensitivity of the potential to the uncertainties in the nuclear densities associated with different models. In this respect we calculate the nucleus-nucleus potential from Millener-Malaguti-Hodgson densities ρ_{WS} [6] and compare with the results derived from ρ_{HF}. The densities ρ_{WS} were derived from single-particle wave functions of a local-state dependent Woods-Saxon potential.

In the next section we give a brief account of the method employed in the calculation of the potential and in section 3 we describe the densities to be used. In section 4 we analyse the influence of different densities on the values taken by the potential in the barrier region. The last section is devoted to conclusions.

2. **The method.** — We calculate the real part of the nucleus-nucleus potential according to the formalism of reference [3] where the potential between two nuclei 1 and 2 was defined as the integral

$$V(R) = \int [H(\rho, \tau) - H(\rho_1, \tau_1) - H(\rho_2, \tau_2)]\, \mathrm{d}\mathbf{r} \quad (1)$$

R being the distance which separates the centres of the interacting nuclei and $H(\rho, \tau)$ is the Skyrme interaction energy density [4].

Some simplifying approximations are used to describe the composite system. In particular the density ρ is treated in the so called *sudden approximation* i.e. ρ is taken as the sum of individual densities which do not change during the collision. The kinetic-energy density is considered in the Thomas-Fermi approximation. Motivations for using these approximations were presented in [7]. For separation distances roughly situated between the sum of the radii of the interacting nuclei and the barrier the Thomas-Fermi approximation allows to include more than 75 % of the exchange effects due to antisymmetrization. However, at the barrier it overestimates the exchange effects and the barrier turns out to be higher than one would expect from an exact treatment of the kinetic energy density.

A somewhat better approximation [8] can be used for the kinetic energy density but for the purpose of this work the Thomas-Fermi approximation seems to be satisfactory.

The use of the Thomas-Fermi approximation reduces the energy density expression $H(\rho, \tau)$ to a function depending on ρ only. Calling it $\overline{H}(\rho)$ the equation (1) becomes :

$$V(R) = \int [\overline{H}(\rho) - \overline{H}(\rho_1) - \overline{H}(\rho_2)]\, \mathrm{d}\mathbf{r}\,, \qquad (2)$$

with

$$\rho = \rho_1 + \rho_2\,. \qquad (3)$$

In fact the expression (2) includes separate contributions from neutrons and protons and to calculate $V(R)$ we need to know $\rho_1^{(n)}$, $\rho_1^{(p)}$, $\rho_2^{(n)}$ and $\rho_2^{(p)}$ i.e. the neutron and proton density of each nucleus.

3. **The densities.** — In the following we describe the densities used in the calculations. Some of their characteristics are given in tables I-III and figures 1-3.

As we have mentioned in the previous section, the ingredients of the calculation are the Skyrme interaction parameters and the neutron and proton densities of the individual nuclei. For the Skyrme interaction parameters we use the set SIII [5] which gives the best overall agreement with the experimental total binding energies and radii of magic nuclei.

To perform our study we make a selection of pairs of magic nuclei mainly among those for which elastic scattering experimental data exist and can give indications on the real part of the potential around the coulomb barrier. The chosen pair are $^{16}O + {}^{16}O$, $^{16}O + {}^{40}Ca$, $^{16}O + {}^{48}Ca$, $^{40}Ca + {}^{40}Ca$, $^{48}Ca + {}^{48}Ca$ and $^{16}O + {}^{208}Pb$.

A consistent choice for the densities of the interacting nuclei would be the Skyrme-Hartree-Fock densities ρ_{HF} [5]. For reasons of simplicity in [3] the calculations were made with Fermi type distributions ρ_F adjusted to reproduce the quantity

$$\rho_{HF} = \rho_{HF}^{(n)} + \rho_{HF}^{(p)}$$

i.e. the sum of neutron and proton Skyrme-Hartree-Fock densities. The neutron and proton densities were therefore assumed to be given by

$$\rho_F^{(n)} = \frac{N}{A}\rho_F\,; \qquad \rho_F^{(p)} = \frac{Z}{A}\rho_F \qquad (4)$$

where

$$\rho_F = \frac{\rho_0}{1 + \exp\left(\dfrac{r - R}{a}\right)} \qquad (4')$$

with parameters given in table I. As a consequence of the relations (4) one has

$$\langle r^2 \rangle_n^{1/2} = \langle r^2 \rangle_p^{1/2} = \langle r^2 \rangle_m^{1/2}$$

i.e. the equality of the neutron, proton and matter r.m.s. radii. The fit is made for ρ_F to reproduce the value of $\langle r^2 \rangle_m^{1/2}$ given by Skyrme-Hartree-Fock calculations and to describe as well as possible the surface region of ρ_{HF}. The values of $\langle r^2 \rangle_n^{1/2}$ or $\langle r^2 \rangle_p^{1/2}$ obtained from this fit and the Hartree-Fock results are reproduced in table II.

TABLE I

Parameters of Fermi type distributions, equation (4'), *which fit Skyrme-Hartree-Fock matter densities*

Nucleus	ρ_0	R	a
^{16}O	0.160 7	2.653 8	0.44
^{40}Ca	0.157 7	3.741 6	0.47
^{48}Ca	0.160 0	3.978 0	0.47
^{208}Pb	0.148 2	6.832 1	0.49

TABLE II

Proton and neutron r.m.s. radii (fm) *given by Skyrme-Hartree-Fock calculations* (HF), *Fermi type distributions* (F) *adjusted to* HF, *and Millener-Malaguti-Hodgson densities* (WS).

	$\langle r^2 \rangle_p^{1/2}$			$\langle r^2 \rangle_n^{1/2}$		
Nucleus	F	HF	WS	F	HF	WS
^{16}O	2.627	2.638	2.671	2.627	2.616	2.690
^{40}Ca	3.384	3.406	3.419	3.384	3.362	3.358
^{48}Ca	3.542	3.461	3.418	3.542	3.599	3.706
^{208}Pb	5.597	5.521	5.434	5.597	5.646	5.621

In the tail region of the densities the differences between the approximation (4) with ρ_F given by (4') and the Skyrme-Hartree-Fock densities of [5] can

be seen in figures 1-3 for ^{16}O, ^{48}Ca and ^{208}Pb respectively. The approximation seems to be quite good for $N = Z$ nuclei (^{40}Ca is not given in the picture) but for the proton densities of $N \neq Z$ nuclei, the approximation $\rho_F^{(p)}$ gives distinctly larger values than $\rho_{HF}^{(p)}$.

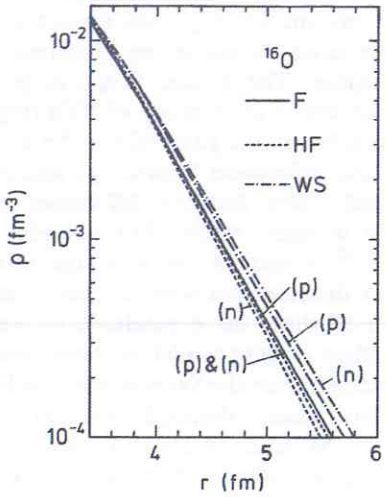

FIG. 1. — The tail of the neutron and proton densities of ^{16}O given by the Fermi type distributions (F) eq. (4), the Skyrme-Hartree-Fock calculations (HF) [5], and Millener-Malaguti-Hodgson model (WS) [6].

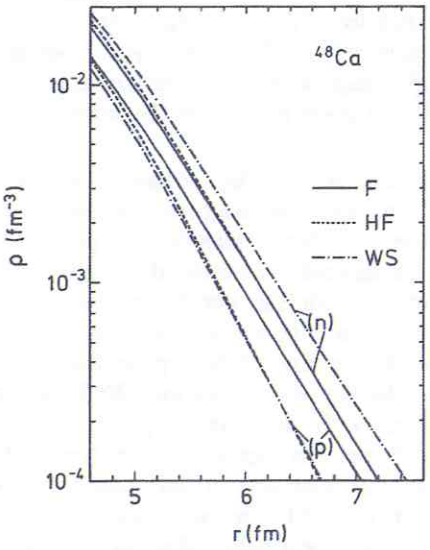

FIG. 2. — Same as figure 1 but for ^{48}Ca.

The third type of densities used in the present calculations are those of reference [6]. They are obtained from single-particle wave functions generated in a local, state dependent potential well of Woods-Saxon shape, and have been successfully applied in several problems, for example the elastic scattering of high energy protons [9].

According to reference [6] the single particle wave function of each occupied state was obtained by

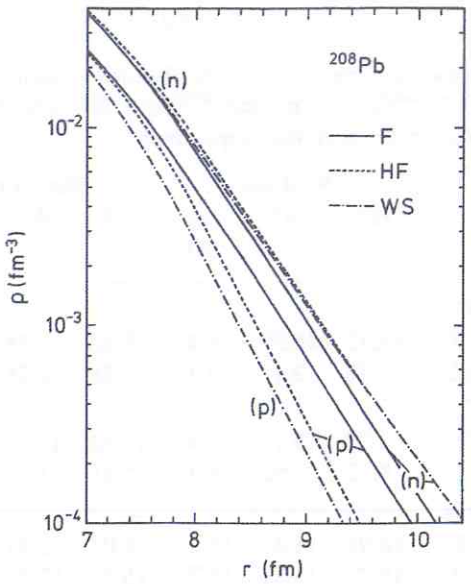

FIG. 3. — Same as figure 1 but for ^{208}Pb.

varying the strength of the central part of the nuclear potentral in order to reproduce as well as possible the corresponding single particle energy if known experimentally. The best fit was obtained for ^{208}Pb (Table IV). For the proton density the constraint of reproducing the experimental charge density radius is also imposed and the success of the fit can be seen in table III. One should remark that the original calculations of reference [6] do not include the centre-of-mass (c.m.) correction. In table III, the r.m.s. radii associated with $\rho_{WS}^{(p)}$ and $\rho_F^{(p)}$ contain this correction evaluated in the following way. Both the centre-of-mass correction and the proton size effect can globally be expressed by the difference

$$\Delta^2 = \langle r^2 \rangle_{ch} - \langle r^2 \rangle_p . \qquad (5)$$

For each nucleus this quantity was estimated from Beiner *et al.* results [5] and added afterwards to the $\langle r^2 \rangle_p$ values associated with $\rho_F^{(p)}$ and $\rho_{WS}^{(p)}$.

TABLE III

Root-mean-square radii (fm) *for the charge distributions of the three different types of densities used in the calculation,* ρ_F, ρ_{HF} *and* ρ_{WS} *as compared to the experiment.*

Nucleus	$\langle r^2 \rangle_{ch}^{1/2}$ F	HF	WS (a)	exp (b)
^{16}O	2.68	2.69	2.73	2.73
^{40}Ca	3.45	3.48	3.49	3.49
^{48}Ca	3.61	3.53	3.49	3.48
^{208}Pb	5.65	5.57	5.49	5.50

(a) Including c.m. corrections (see text). The original numbers are 2.75, 3.51, and 5.49 respectively.
(b) As in reference [5].

TABLE IV

Single particle energies of the last occupied levels of ^{16}O, ^{40}Ca, ^{48}Ca, *and* ^{208}Pb : HF *and* WS *are results of* [5] *and* [6] *respectively.*

	Protons			Neutrons		
	HF	WS	exp (*)	HF	WS	exp (*)
	—	—	—	—	—	—
^{16}O						
1p 3/2	16.12	16.99	18.4	19.62	17.18	21.8
1p 1/2	10.18	12.14	12.1	13.58	12.38	15.7
^{40}Ca						
2s 1/2	8.37	9.12	10.9	15.52	14.87	18.1
1d 3/2	8.12	7.92	8.3	15.11	13.72	15.6
^{48}Ca						
2s 1/2	14.91	15.41	15.3	16.03	12.73	12.55
1d 3/2	15.87	15.51	15.7	15.7	11.48	12.52
1f 7/2				9.6	9.71	9.94
^{208}Pb						
1g 9/2	17.27	15.43	15.43			
1g 7/2	13.5	11.43	11.43			
2d 5/2	10.19	9.70	9.70			
1h 11/2	9.56	9.37	9.37			
2d 3/2	8.42	8.38	8.38			
3s 1/2	7.27	8.03	8.03			
1h 9/2				12.55	10.85	10.85
2f 7/2				11.12	9.72	9.72
1i 13/2				10.09	9.01	9.01
3p 3/2				8.04	8.27	8.27
2f 5/2				8.33	7.95	7.95
3p 1/2				7.02	7.38	7.38

(*) See reference [10].

The tails of the $\rho_{WS}^{(p)}$ and $\rho_{WS}^{(n)}$ densities are drawn in figures 1-3. For all nuclei there are differences between the Skyrme-Hartree-Fock densities and Millener-Malaguti-Hodgson densities which could be related to the differences in the fit of the single particle energies of the last occupied states (Table IV).

In the next section we shall see the influence of these differences on the values of nucleus-nucleus potential around the barrier region.

4. **The potential.** — In this section we present and compare the potentials we have obtained for the three different densities described in the previous section. We are interested in the barrier region only. There the nuclear interaction results from the overlap of the density tails.

In table V we give results for the pairs $^{16}O + ^{48}Ca$, $^{48}Ca + ^{48}Ca$, and $^{16}O + ^{208}Pb$. For pairs such as $^{16}O + ^{16}O$, $^{16}O + ^{40}Ca$ and $^{40}Ca + ^{40}Ca$ the discussion is similar to the case $^{16}O + ^{48}Ca$.

In all cases but $^{16}O + ^{208}Pb$ the potential obtained from the Skyrme-Hartree-Fock densities is less attractive in the tail region than the potential obtained from the Fermi type distributions adjusted to reproduce ρ_{HF}. For $^{16}O + ^{208}Pb$ there is practically no difference. The largest difference appears for $^{48}Ca + ^{48}Ca$ where the V_{HF} is approximately 15 % higher than V_F around the barrier and the barrier position is situated by 0.1 fm inward for V_{HF} with respect to V_F while in the other cases the barrier position remains practically the same. The reason is the large difference between the tails of $\rho_F^{(p)}$ and $\rho_{HF}^{(p)}$ of ^{48}Ca (Fig. 2) which doubles its effect in the pair $^{48}Ca + ^{48}Ca$. For ^{208}Pb there are also differences between ρ_F and ρ_{HF} but the neutron and proton densities differences compensate each other to some extent. For non-identical pairs as $^{16}O + ^{208}Pb$ there is also a compensation of differences of densities between the two nuclei.

In order to study the dependence of the potential on the nuclear density model we have compared the results obtained from the Skyrme-Hartree-Fock densities V_{HF} with those obtained from the shell-model densities of Millener-Malaguti-Hodgson V_{WS}. The ratio V_{HF}/V_{WS} at values of R around the barrier region of each pair varies from ~ 0.75 for $^{16}O + ^{16}O$ to 1.02 for $^{16}O + ^{208}Pb$. This is in qualitative agreement with the difference observed in the density tails. From figures 1-3 one can see that $\rho_{WS}^{(n)} - \rho_{HF}^{(n)}$ is positive and significantly large for ^{16}O and ^{48}Ca and negligible for ^{208}Pb. As far as the proton densities are concerned the $\rho_{WS}^{(p)}$ are slightly larger than $\rho_{HF}^{(p)}$ for ^{16}O, very similar for ^{48}Ca and smaller for ^{208}Pb, so that for the pair $^{16}O + ^{208}Pb$ the larger overlap of $\rho_{WS}^{(n_1)}$ and $\rho_{WS}^{(n_2)}$ compensates the smaller overlap of $\rho_{WS}^{(p_1)}$ and $\rho_{WS}^{(p_2)}$ and gives practically the same results as for ρ_{HF}.

The sensitivity of the potential to the density distributions used has also been discussed by Fleckner and Mosel [11], for a selection of pairs. The same order of magnitude is obtained for the variation of the potential with the density model.

Within our method we have also studied the dependence of the nucleus-nucleus potential on the parameters of the Skyrme interaction. We have performed calculations with the sets of parameters SIV and SV [5] and the corresponding neutron and proton densities. For these sets of parameters the potential gets higher by 20-30 % in light systems at the barrier.

In order to have a better idea concerning the differences between V_F, V_{HF} and V_{WS} we have calculated the elastic scattering cross section σ/σ_R for each of these potentials and in figure 4 we show the case of $^{16}O + ^{48}Ca$ at $E_{lab} = 40$ MeV. The calculations were performed with Raynal's code MAGALI. The calculated real potential was approximated by a Woods-Saxon shape with parameters given in table VI. This parametrized shape reproduces the potential between the inflexion point and the barrier with an error smaller than 1 %.

We extrapolate the Woods-Saxon shape to smaller separation distances because here we discuss a strong

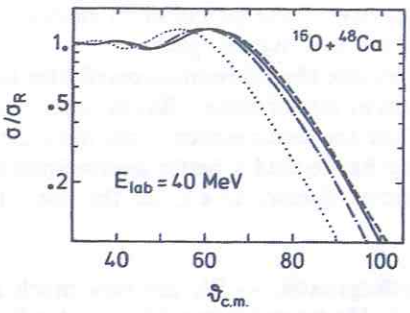

FIG. 4. — The elastic scattering cross-section for $^{16}O + ^{48}Ca$, et $E_{lab} = 40$ MeV. The dotted curve is the phenomenological fit [12], the dashed curve is obtained from V_{HF}, the full curve from V_F the dot — and — dash curve from V_{WS}.

TABLE VI

Parametrization of the $^{16}O + ^{48}Ca$ calculated potential V_F, V_{HF}, and V_{WS} with a Woods-Saxon shape (V_0, R_0, T)

Potential	V_0 (MeV)	R_0 (fm)	T (fm)	W (MeV)	θ_c (deg)
—	—	—	—	—	—
V_F	− 36.52	7.1	0.582	9.2	89.5
V_{HF}	− 35.97	7.13	0.564	8.6	90.5
V_{WS}	− 39.04	7.1	0.600	10.7	87.0

The strength W of the imaginary part used in the calculation of the cross section (Fig. 4) and the resulting critical angle θ_c (see text) are also indicated.

absorption case (Fresnel diffraction pattern) where the elastic scattering cross section at forward angles is independent of the values taken by the potential at short separation distances [2]. Furthermore the detailed shape of the imaginary part is not important and therefore for the imaginary part we choose a volume absorption with the geometry of the real part and a variable strength W. The values of W are adjusted to reproduce the maximum height of the Fresnel diffraction pattern and they are also given in table VI. In the same table the grazing angle θ_c is indicated. This is the angle for which $\sigma/\sigma_R \simeq 0.25$. For completeness we mention that $\theta_c^{exp} \simeq 80.5°$ [12]. The largest discrepancy with respect to the experiment appear for V_{HF} where $\theta_c^{(HF)} = 90.5°$.

It was shown elsewhere how this discrepancy could be reduced to a large extent [8]. Here we are interested in the difference produced by the density models.

The difference between $\theta_c^{(F)} = 89.5°$ and $\theta_c^{(HF)}$ is very small and by an appropriate change in the surface absorption one could remove it. In this way one can also diminish the difference between $\theta_c^{(WS)} = 87°$ and $\theta_c^{(F)}$ or $\theta_c^{(HF)}$. But by the same procedure one can not change the position of the main peak in the cross section and therefore the angle at which this peak is situated would provide an additional test for the real part. Hence very precise measurements are necessary in the region of this peak.

5. **Conclusions.** — We have calculated the real part of the nucleus-nucleus potential using a method based on the Skyrme interaction energy functional and compared the results obtained from three different nuclear densities : Skyrme-Hartree-Fock densities of reference [5], Fermi type distributions adjusted to the Skyrme-Hartree-Fock densities and shell-model-densities of reference [6]. We have studied the effect of the differences in the tail densities i.e. the region where the density takes values between

$$10^{-2}\ \text{fm}^{-3} \quad \text{and} \quad 10^{-4}\ \text{fm}^{-3}.$$

One can conclude that the approximation of the

TABLE V

Values of the nucleus-nucleus potential

	$^{16}O + ^{48}Ca$				$^{48}Ca + ^{48}Ca$				$^{16}O + ^{208}Pb$			
R	V_F	V_{HF}	V_{WS}	R	V_F	V_{HF}	V_{WS}	R	V_F	V_{HF}	V_{WS}
—	—	—	—	—	—	—	—	—	—	—	—
7.8	− 8.38	− 8.41	− 9.24	8.6	− 19.62	− 18.70	− 18.88	9.8	− 24.76	− 25.06	− 24.41
8.0	− 6.40	− 6.37	− 7.13	8.8	− 15.90	− 15.04	− 15.26	10.0	− 20.77	− 21.06	− 20.35
8.2	− 4.81	− 4.73	− 5.41	9.0	− 12.62	− 11.80	− 12.05	10.2	− 17.00	− 17.20	− 16.60
8.4	− 3.55	− 3.45	− 4.04	9.2	− 9.83	− 9.05	− 9.32	10.4	− 13.62	− 13.77	− 13.26
8.6	− 2.59	− 2.48	− 2.98	9.4	− 7.52	− 6.78	− 7.07	10.6	− 10.69	− 10.79	− 10.39
8.7	− 2.20	− 2.09	− 2.54	9.6	− 5.66	− 4.99	− 5.26	10.8	− 8.23	− 8.28	− 8.01
8.8	− 1.86	− 1.76	− 2.16	9.8	− 4.20	− 3.60	− 3.85	11.0	− 6.24	− 6.25	− 6.07
8.9	− 1.57	− 1.50	− 1.84	9.9	− 3.60	− 3.04	− 3.27	11.1	− 5.40	− 5.39	− 5.26
9.0	− 1.32	− 1.23	− 1.56	10.0	− 3.07	− 2.56	− 2.77	11.2	− 4.66	− 4.64	− 4.54

R is the distance separating the centres of the nuclei. V_F, V_{HF} and V_{WS} are the results obtained with ρ_F, ρ_{HF} and ρ_{WS} respectively. The value of the potential at the barrier is underlined.

Skyrme-Hartree-Fock densities with Fermi type distributions is satisfactory in general, either due to the quality of the approximation itself for $N = Z$ nuclei or due to the compensation of different contributions. The typical difference of 5 % between V_{HF} and V_F in the barrier region accounts for a difference of 1°-1.5° in the critical angle if the imaginary part is chosen to have the same geometry as the real part. This difference can be removed by a proper choice of the surface absorption.

From the comparison between the results based on Beiner *et al.* densities [5] and Millener-Malaguti-Hodgson densities [6] we can conclude that the latter seems to give somewhat better results than the former. The sensitivity of the potential to nuclear densities increases towards lighter pairs.

Therefore one should be more careful for the choice of densities of lighter nuclei. But in order to substantially reduce the disagreement with the experimental results one has to find a better approximation to the kinetic energy density as e.g. on the lines described in [8].

Acknowledgments. — We are very much indebted to Dr. P. E. Hodgson for providing us detailed results for the shell-model single particle densities and for useful discussions. Computational help from Miss J. Garbar is gratefully acknowledged.

References

[1] ALEXANDER, J. M., DELAGRANGE, H. and FLEURY, A., *Phys. Rev.* C **12** (1975) 149.
[2] SATCHLER, G. R., Proceedings of the Conference *Reactions Between Complex Nuclei*, ed. Robinson R. L., McGowan F. K., Ball J. B., and Hamilton J. H. (North-Holland, Amsterdam) 1974, p. 171 ; BALL, J. B. *et al.*, *Nucl. Phys.* A **252** (1975) 208.
[3] STANCU, Fl. and BRINK, D. M., *Nucl. Phys.* A **270** (1976) 236.
[4] VAUTHERIN, D. and BRINK, D. M., *Phys. Rev.* C **5** (1972) 626.
[5] BEINER, M. *et al.*, *Nucl. Phys.* A **238** (1975) 29.
[6] MILLENER, D. J. and HODGSON, P. E., *Nucl. Phys.* A **209** (1973) 59 ; MALAGUTI, F. and HODGSON, P. E., *Nucl. Phys.* A **215** (1973) 243 ; HODGSON, P. E., private communication.
[7] BRINK, D. M. and STANCU, Fl., *Nucl. Phys.* A **243** (1975) 175.
[8] STANCU, Fl., Proceedings of the International Workshop on Gross Properties of Nuclei and Nuclear Excitations V, Hirschegg, Jan. 17-22, 1977 (Inst. für Kernphysik, Technische Hochschule Darmstadt, 1977).
[9] KUJAWSKI, E. and VARY, J. P., *Phys. Rev.* C **12** (1975) 1271.
[10] BOHR, A. and MOTTELSON, B., *Nuclear Structure* (Benjamin, New York) 1969, vol. 1.
[11] FLECKNER, J. and MOSEL, U., *Nucl. Phys.* A **277** (1977) 170.
[12] GROENEWELD, K. O. *et al.*, *Phys. Rev.* C **6** (1972) 805.